

# Improved $(g - 2)_\mu$ Measurements and Supersymmetry: Implications for $e^+e^-$ colliders

MANIMALA CHAKRABORTI<sup>1\*</sup>, SVEN HEINEMEYER<sup>2,3,4</sup> AND IPSITA SAHA<sup>5</sup>

<sup>1</sup>*Astrocent, Nicolaus Copernicus Astronomical Center of the Polish Academy of Sciences,  
ul. Rektorska 4, 00-614 Warsaw, Poland*

<sup>2</sup>*Instituto de Física Teórica (UAM/CSIC), Universidad Autónoma de Madrid,  
Cantoblanco, 28049, Madrid, Spain*

<sup>3</sup>*Campus of International Excellence UAM+CSIC, Cantoblanco, 28049, Madrid, Spain*

<sup>4</sup>*Instituto de Física de Cantabria (CSIC-UC), 39005, Santander, Spain*

<sup>5</sup>*Kavli IPMU (WPI), UTIAS, University of Tokyo, Kashiwa, Chiba 277-8583, Japan*

## Abstract

The persistent  $3 - 4\sigma$  discrepancy between the experimental result from BNL for the anomalous magnetic moment of the muon,  $(g - 2)_\mu$ , and its Standard Model (SM) prediction, was confirmed recently by the “MUON G-2” result from Fermilab. The combination of the two measurements yields a deviation of  $4.2\sigma$  from the SM value. Here, we review an analysis of the parameter space of the electroweak (EW) sector of the Minimal Supersymmetric Standard Model (MSSM), which can provide a suitable explanation of the anomaly while being in full agreement with other latest experimental data like the direct searches for EW particles at the LHC and dark matter (DM) relic density and direct detection constraints. Taking the lightest supersymmetric particle (LSP) (the lightest neutralino in our case) to be the DM candidate, we discuss the case of a mixed bino/wino LSP, which can account for the full DM relic density of the universe and that of wino and higgsino DM, where we take the relic density only as an upper bound. We observe that an upper limit of  $\sim 600$  GeV can be obtained for the LSP and next-to (N)LSP masses establishing clear search targets for the future HL-LHC EW searches, but in particular for future high-energy  $e^+e^-$  colliders, such as the ILC or CLIC.

---

\*Talk presented at the International Workshop on Future Linear Colliders (LCWS2021), 15-18 March 2021. C21-03-15.1.

# 1 Introduction

While the LHC is yet to find any sign of new physics, indirect searches such as, low-energy experiments, astrophysical measurements etc. are providing crucial hints of beyond the SM (BSM) scenarios. Specifically, the sustained deviation of  $3\text{--}4\sigma$  in the anomalous magnetic moment of muon,  $(g-2)_\mu$ , between the theoretical prediction of the SM [1] (see Ref. [2] for a full list of references) and the experimental observation by the Brookhaven National Laboratory (BNL) [3] has long been standing in support of new physics scenario. The BNL measurement,

$$a_\mu^{\text{BNL}} = 11659209.1(5.4)(3.3) \times 10^{-10} , \quad (1)$$

when compared with the SM prediction

$$a_\mu^{\text{SM}} = (11659181.0 \pm 4.3) \times 10^{-10} , \quad (2)$$

leads to a deviation of

$$\Delta a_\mu^{\text{old}} = (28.1 \pm 7.6) \times 10^{-10} , \quad (3)$$

corresponding to a  $\sim 3.7\sigma$  discrepancy. The new result from Fermilab “MUON G-2” collaboration [4] was announced recently [5], which is within  $0.8\sigma$  in agreement with the older BNL result on  $(g-2)_\mu$ . The combination of the two results was given as

$$a_\mu^{\text{exp}} = (11659206.1 \pm 4.1) \times 10^{-10} , \quad (4)$$

yielding a new deviation from the SM prediction of

$$\Delta a_\mu^{\text{new}} = (25.1 \pm 5.9) \times 10^{-10} , \quad (5)$$

corresponding to a discrepancy of  $4.2\sigma$ .

This result particularly upholds one of the leading candidates of BSM theories, the Minimal Supersymmetric Standard Model (MSSM) [6–9]. The deviation in Eq. (5) can easily be explained in the realm of MSSM scenario with electroweak (EW) supersymmetric (SUSY) particle masses around a few hundred GeV. However, in view of the stringent constraints on EW SUSY particles from the direct searches at the LHC, it is essential to perform a comprehensive analysis including both the  $(g-2)_\mu$  result as well as the latest constraints on neutralinos, charginos and sleptons from the LHC. On the other hand, the R-parity conserving MSSM naturally predicts a suitable Dark Matter (DM) candidate in terms of the lightest neutralino as the lightest SUSY particle (LSP) [10, 11]. Therefore, it seems only natural to include the experimental constraint on the DM density and limits from direct detection in the analysis to further constrain the parameter space of our interest.

In these proceedings, following Refs. [2, 12, 13], we review the mass ranges of EW superpartners that can successfully explain the  $(g-2)_\mu$  anomaly while being in agreement with all the relevant experimental data. In Refs. [12, 13] we employed the constraint coming from Eq. (3) to constraint the EW MSSM parameter space. An updated analysis using the latest experimental world average can be found in Ref. [2], where we show that the new  $(g-2)_\mu$  result (Eq. (5)) confirms the predictions made in Ref. [12] concerning the upper limits on

the masses of the (next-to-) lightest SUSY particles. We include the latest LHC searches via recasting in **CheckMATE** [14–16]. For the DM, we consider two main scenarios depending on whether the LSP can account for the full relic density or it can be only a subdominant component of the total DM content of the universe. For the former scenario, we consider a mixed bino/wino LSP while the latter opens up the possibility of wino and higgsino DM. We observe that the combined data helps to narrow down the allowed parameter region, providing clear targets for possible future  $e^+e^-$  colliders, such as the ILC [17, 18] or CLIC [18, 19].

## 2 The EW sector of MSSM

We give a very brief description of the EW sector of MSSM, consisting of charginos, neutralinos and sleptons. The masses and mixings of the charginos and neutralinos are determined by  $U(1)_Y$  and  $SU(2)_L$  gaugino masses  $M_1$  and  $M_2$ , the Higgs mixing parameter  $\mu$  and the ratio of the two vacuum expectation values (vevs) of the two Higgs doublets of MSSM,  $\tan\beta = v_2/v_1$ . This results in four neutralinos and two charginos with the mass ordering  $m_{\tilde{\chi}_1^0} < m_{\tilde{\chi}_2^0} < m_{\tilde{\chi}_3^0} < m_{\tilde{\chi}_4^0}$  and  $m_{\tilde{\chi}_1^\pm} < m_{\tilde{\chi}_2^\pm}$ . Considering the size and sign of the anomaly, it is sufficient for our analysis to focus on positive values of  $M_1$ ,  $M_2$  and  $\mu$  [12]. For the sleptons, we choose common soft SUSY-breaking parameters for all three generations,  $m_{\tilde{l}_L}$  and  $m_{\tilde{l}_R}$ . We take the trilinear coupling  $A_l$  ( $l = e, \mu, \tau$ ) to be zero for all the three generations of leptons. In general we follow the convention that  $\tilde{l}_1$  ( $\tilde{l}_2$ ) has the large “left-handed” (“right-handed”) component. The symbols equal for all three generations,  $m_{\tilde{l}_1}$  and  $m_{\tilde{l}_2}$ , but we also refer to scalar muons directly,  $m_{\tilde{\mu}_1}$  and  $m_{\tilde{\mu}_2}$ .

Following the stronger experimental limits from the LHC [20, 21], we assume that the colored sector of the MSSM is sufficiently heavier than the EW sector, and does not play a role in this analysis. For the Higgs-boson sector we assume that the radiative corrections originating largely from the top/stop sector brings the light  $\mathcal{CP}$ -even Higgs boson mass in the experimentally observed region,  $M_h \sim 125$  GeV. This naturally yields stop masses in the TeV range [22, 23], in agreement with the above assumption. We have not considered  $\mathcal{CP}$ -violation in this study, i.e. all parameters are real.  $M_A$  has also been set to be above the TeV scale. Consequently, we do not include explicitly the possibility of  $A$ -pole annihilation, with  $M_A \sim 2m_{\tilde{\chi}_1^0}$ . Similarly, we do not consider  $h$ - or  $Z$ -pole annihilation (see, e.g., Ref. [24]), as such a light neutralino sector likely overshoots the  $(g-2)_\mu$  contribution [12].

## 3 Relevant constraints

The most important constraint that we consider comes from the  $(g-2)_\mu$  result. We use Eq. (5) (and in some older results also Eq. (3)) as a cut at the  $\pm 2\sigma$  level. However, it is worth mentioning here that we did not take into account the results of the new lattice calculation for the leading order hadronic vacuum polarization (LO HVP) contribution [25], which have also not been used in the new theory world average, Eq. (2) [1], but would certainly lead to significant change in our conclusion if turns out to be true, see also the discussions in Refs. [26–28].

We remind that the main contribution to  $(g-2)_\mu$  in MSSM at the one-loop level comes from diagrams involving  $\tilde{\chi}_1^\pm - \tilde{\nu}$  and  $\tilde{\chi}_1^0 - \tilde{\mu}$  loops. In our analysis the MSSM contribution to

$(g-2)_\mu$  at two loop order is calculated using `GM2Calc` [29], implementing two-loop corrections from [30–32] (see also [33, 34]).

Various other constraints that are taken into account comprises the following:

- **Vacuum stability constraints:** All points are checked to possess a stable and correct EW vacuum, e.g. avoiding charge and color breaking minima, using the public code `Evade` [35, 36].
- **Constraints from the LHC:** All relevant EW SUSY searches are taken into account, mostly via `CheckMATE` [14–16], where many analyses had to be implemented newly [12]. We also take into account the latest constraints from the disappearing track searches at the LHC [37, 38]. These become particularly important for wino DM scenario where the mass gap between  $\tilde{\chi}_1^\pm$  and  $\tilde{\chi}_1^0$  can be  $\sim$  a few hundred MeV.
- **Dark matter relic density and direct detection constraints:** We use the latest result from Planck [39].

$$\Omega_{\text{CDM}} h^2 = 0.120 \pm 0.001. \quad (6)$$

For the wino and higgsino DM cases, we take the relic density as an *upper* limit (evaluated from the central value plus  $2\sigma$ ). The relic density in the MSSM is evaluated with `MicrOMEGAs` [40–43].

We employ the constraint on the spin-independent DM scattering cross-section  $\sigma_p^{\text{SI}}$  from XENON1T [44], evaluating the theoretical prediction using `MicrOMEGAs`. For parameter points with  $\Omega_{\tilde{\chi}} h^2 \leq 0.118$  ( $2\sigma$  lower limit from Planck [39]), we scale the cross-section with a factor of  $(\Omega_{\tilde{\chi}} h^2 / 0.118)$  to account for the fact that  $\tilde{\chi}_1^0$  provides only a fraction of the total DM relic density of the universe.

## 4 Parameter scan

We scan the relevant MSSM parameter space to obtain lower and *upper* limits on the lightest neutralino, chargino and slepton masses. The three scan regions that cover the complete parameter space under consideration are as given below:

**(A) bino/wino DM with  $\tilde{\chi}_1^\pm$ -coannihilation:**

$$\begin{aligned} 100 \text{ GeV} &\leq M_1 \leq 1 \text{ TeV}, & M_1 &\leq M_2 \leq 1.1 M_1, \\ 1.1 M_1 &\leq \mu \leq 10 M_1, & 5 &\leq \tan \beta \leq 60, \\ 100 \text{ GeV} &\leq m_{\tilde{l}_L} \leq 1 \text{ TeV}, & m_{\tilde{l}_R} &= m_{\tilde{l}_L}. \end{aligned} \quad (7)$$

**(B) Higgsino DM:**

$$\begin{aligned} 100 \text{ GeV} &\leq \mu \leq 1.2 \text{ TeV}, & 1.1 \mu &\leq M_1 \leq 10 \mu, \\ 1.1 \mu &\leq M_2 \leq 10 \mu, & 5 &\leq \tan \beta \leq 60, \\ 100 \text{ GeV} &\leq m_{\tilde{l}_L}, m_{\tilde{l}_R} \leq 2 \text{ TeV}. \end{aligned} \quad (8)$$

### (C) Wino DM

$$\begin{aligned}
100 \text{ GeV} \leq M_2 \leq 1.5 \text{ TeV} , \quad 1.1M_2 \leq M_1 \leq 10M_2 , \\
1.1M_2 \leq \mu \leq 10M_2, \quad 5 \leq \tan \beta \leq 60, \\
100 \text{ GeV} \leq m_{\tilde{t}_L}, m_{\tilde{t}_R} \leq 2 \text{ TeV} .
\end{aligned} \tag{9}$$

In all the scans we choose flat priors of the parameter space and generate  $\mathcal{O}(10^7)$  points. We use **SuSpect** [45] as spectrum and SLHA file generator. The points are required to satisfy the  $\tilde{\chi}_1^\pm$  mass limit from LEP [46]. The SLHA output files from **SuSpect** are then passed as input to **GM2Calc** and **MicrOMEGAs** for the calculation of  $(g-2)_\mu$  and the DM observables, respectively. The parameter points that satisfy the  $(g-2)_\mu$  and DM constraint, and additionally the vacuum stability constraints checked with **Evade** are then passed to the final step to be checked against the latest LHC constraints implemented in **CheckMATE**. The branching ratios of the relevant SUSY particles are computed using **SDECAY** [47] and given as input to **CheckMATE**.

## 5 Results

In this section we review some of the results for the scenarios defined above [2, 12, 13]. We follow the analysis flow as described above and denote the points surviving certain constraints with different colors:

- grey (round): all scan points.
- green (round): all points that are in agreement with  $(g-2)_\mu$ .
- blue (triangle): points that additionally give the correct relic density.
- cyan (diamond): points that additionally pass the DD constraints.
- red (star): points that additionally pass the LHC constraints.

In Fig. 1 we show our results for the bino/wino  $\tilde{\chi}_1^\pm$ -coannihilation scenario in the  $m_{\tilde{\chi}_1^0}$ - $m_{\tilde{\chi}_1^\pm}$  (left) and  $m_{\tilde{\chi}_1^0}$ - $m_{\tilde{t}_1}$  (right) planes [2]. Starting with the  $(g-2)_\mu$  constraint (Eq. (5)) (green points) in the  $m_{\tilde{\chi}_1^0}$ - $m_{\tilde{\chi}_1^\pm}$  plane, one can observe a clear upper limit of about 700 GeV. Applying the CDM constraints reduce the upper limit further. The LHC constraints, corresponding to the “surviving” red points (stars), do not yield a further reduction from above, but cut (as anticipated) only points in the lower mass region. The LHC constraint which is effective in this parameter plane is the one designed for compressed spectra [48]. Other LHC constraint that is effective in this case is the bound from slepton pair production leading to dilepton and  $\cancel{E}_T$  in the final state [49]. Thus, the experimental data set an upper as well as a lower bound, yielding a clear search target for the upcoming LHC runs, and in particular for future  $e^+e^-$  colliders.

The distribution of the lighter slepton mass (where it should be kept in mind that we have chosen the same masses for all three generations), as in the  $m_{\tilde{\chi}_1^0}$ - $m_{\tilde{t}_1}$  plane, is shown in the right plot of Fig. 1. The  $(g-2)_\mu$  constraint is satisfied in a triangular region with its tip

around  $(m_{\tilde{\chi}_1^0}, m_{\tilde{l}_1}) \sim (700 \text{ GeV}, 800 \text{ GeV})$ . This is slightly reduced when the DM constraints are taken into account. The LHC constraints cut out lower slepton masses, going up to  $m_{\tilde{l}_1} \lesssim 400 \text{ GeV}$ , as well as part of the very low  $m_{\tilde{\chi}_1^0}$  points nearly independent of  $m_{\tilde{l}_1}$ . Details on these cuts can be found in Ref. [12].

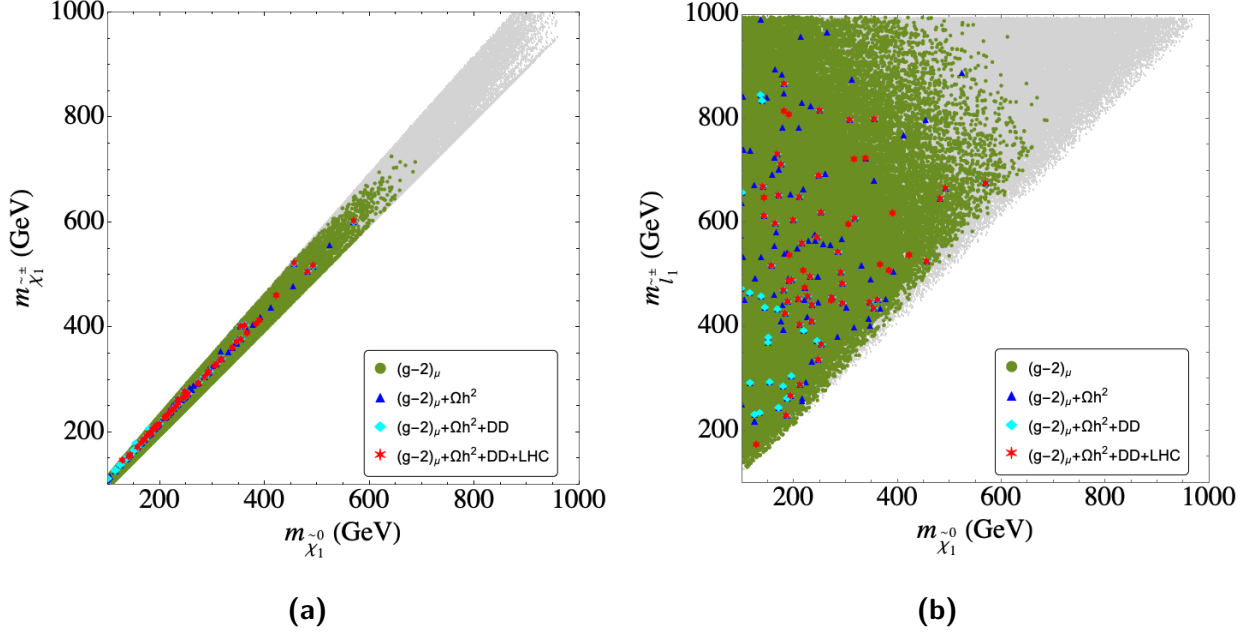


**Figure 1:** The results of our parameter scan for the bino/wino  $\tilde{\chi}_1^\pm$ -coannihilation scenario in the  $m_{\tilde{\chi}_1^0}$ - $m_{\tilde{\chi}_1^\pm}$  plane (left) and  $m_{\tilde{\chi}_1^0}$ - $m_{\tilde{l}_1}$  plane (right). For the color coding: see text.

Our results for the higgsino and wino DM scenarios are presented in Fig. 2 [13]. We show our results in the  $m_{\tilde{\chi}_2^0}$ - $\Delta m (= m_{\tilde{\chi}_2^0} - m_{\tilde{\chi}_1^0})$  plane for the higgsino DM scenario (left) and in the  $m_{\tilde{\chi}_1^\pm}$ - $\Delta m (= m_{\tilde{\chi}_1^\pm} - m_{\tilde{\chi}_1^0})$  plane for the wino DM scenario (right), where the  $(g-2)_\mu$  limit here corresponds to Eq. (3). No green points are visible in these plots as all the points that pass the  $(g-2)_\mu$  constraint are also in agreement with the DM relic density constraint, resulting in only blue points. For the higgsino DM case, we also explicitly show the constraint from compressed spectra searches [48] as a black line<sup>1</sup>. In the case of wino DM the relevant LHC constraint are the disappearing track searches [37, 38], due to the relatively long life-time of the NLSP, the light chargino. In both scenarios the combination of  $(g-2)_\mu$ , DM limits and LHC searches put an upper limit on the (N)LSP masses. They are found at  $\sim 500(600) \text{ GeV}$  for higgsino (wino) DM. As for the case of bino/wino DM, clear search targets are set for future LHC runs, and in particular for the ILC and CLIC. For a more detailed description of these two scenarios see Ref. [13].

<sup>1</sup>This is an updated plot compared to Ref. [13] due to a small correction in the determination of the compressed search limits.

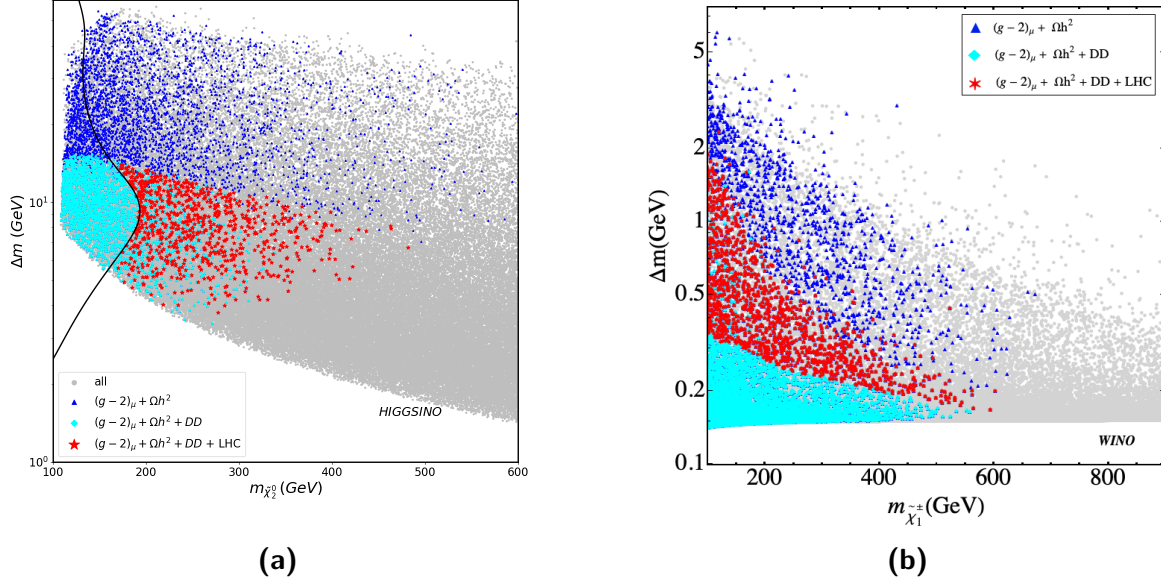


**Figure 2:** The results of our parameter scan in the  $m_{\tilde{\chi}_2^0}$ - $\Delta m (= m_{\tilde{\chi}_2^0} - m_{\tilde{\chi}_1^0})$  plane for the higgsino DM scenario (left) and  $m_{\tilde{\chi}_1^\pm}$ - $\Delta m (= m_{\tilde{\chi}_1^\pm} - m_{\tilde{\chi}_1^0})$  plane for the wino DM scenario (right)  $((g-2)_\mu$  limits from Eq. (3)). For the color coding: see text.

## 6 Future linear collider prospects

In this section we briefly discuss the prospects for the direct detection of the (relatively light) EW particles at possible future  $e^+e^-$  colliders such as ILC [17, 18] or CLIC [18, 19], which can reach energies up to 1 TeV and 3 TeV, respectively. We evaluate the cross-sections for various SUSY pair production modes for the energies currently foreseen in the run plans of the two colliders. The anticipated energies and integrated luminosities are listed in Tab. 1. The cross-section predictions are based on tree-level results, obtained as in [50, 51], where it was shown that the full one-loop corrections can amount up to 10-20%<sup>2</sup>. We do not attempt any rigorous experimental analysis, but follow the idea that to a good approximation, final states with the sum of the masses smaller than the center-of-mass energy can be detected [53–55]. We also note that in case of several EW SUSY particles in reach of an  $e^+e^-$  collider, large parts of the overall SUSY spectrum can be measured and fitted [56].

In Fig. 3 we show the cross-section predictions for  $e^+e^- \rightarrow \tilde{\chi}_1^\pm \tilde{\chi}_1^\mp$  (left) and  $e^+e^- \rightarrow \tilde{\mu}_1 \tilde{\mu}_1$  (right) in the bino/wino  $\tilde{\chi}_1^\pm$ -coannihilation case as a function of the sum of the final state masses [12]. The points shown in different shades of green (violet) indicate the cross-sections at the various ILC (CLIC) energies. All shown points (open and filled) are in agreement with the old  $(g-2)_\mu$  result, see Eq. (3) (Filled circles indicate a hypothetical future measurement as discussed in Ref. [12]). Using the updated result, Eq. (5) would not change this picture in a relevant way. The upper limits on  $m_{\tilde{\chi}_1^0}$  of about 570 GeV for the old (and new)  $(g-2)_\mu$  constraint implies that with  $\sqrt{s} = 1000$  GeV a considerable part of the allowed region can be

<sup>2</sup>Evaluation of the full one-loop corrections as in [50, 51] would require the determination of the preferred renormalization scheme for each point individually (see [52] for details).

Collider	$\sqrt{s}$ [GeV]	$\mathcal{L}_{\text{int}}$ [ $\text{ab}^{-1}$ ]	Collider	$\sqrt{s}$ [GeV]	$\mathcal{L}_{\text{int}}$ [ $\text{ab}^{-1}$ ]
ILC	250	2	CLIC	380	1
	350	0.2		1500	2.5
	500	4		3000	5
	1000	8			

**Table 1:** Anticipated center-of-mass energies,  $\sqrt{s}$  and corresponding integrated luminosities,  $\mathcal{L}_{\text{int}}$  at ILC [57, 58] and CLIC [59] (as used in [60]).

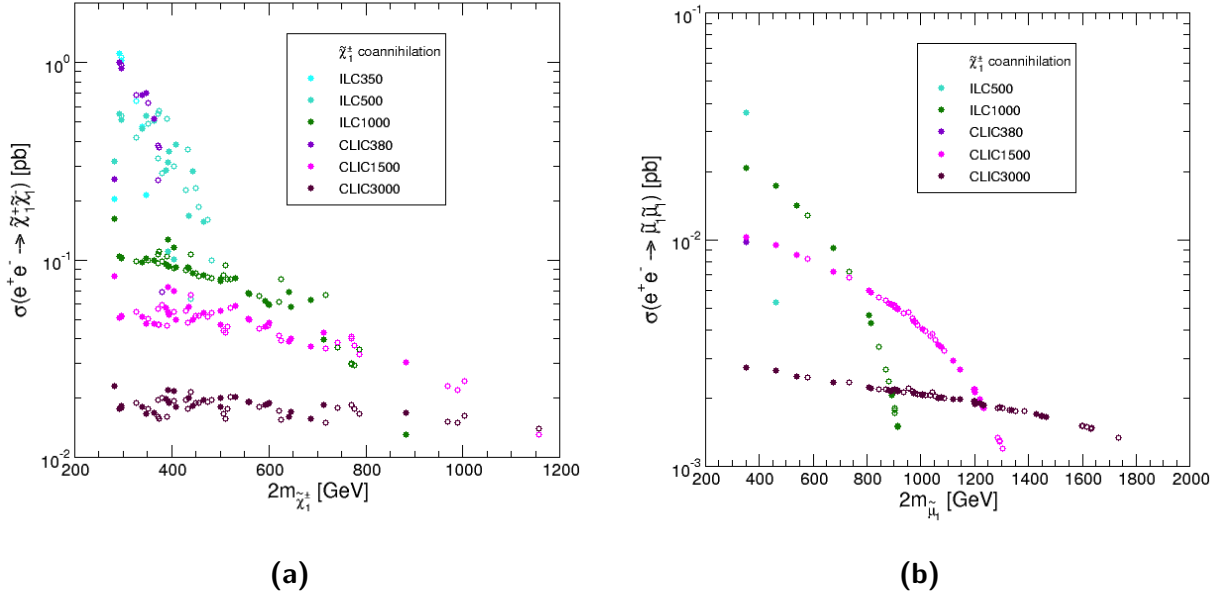


**Figure 3:** cross-section predictions for  $e^+e^- \rightarrow \tilde{\chi}_1^\pm \tilde{\chi}_1^\mp$  (left) and  $e^+e^- \rightarrow \tilde{\mu}_1 \tilde{\mu}_1$  (right) for the bino/wino  $\tilde{\chi}_1^\pm$ -coannihilation case at the ILC and CLIC as a function of the sum of the final state masses. Open (filled) circles: see text.

covered. The reach could become even stronger in the case of the future  $(g-2)_\mu$  constraint. With the same central value but only slightly better precision the upper limits on  $m_{\tilde{\chi}_1^0}$  go down to  $\sim 450$  GeV, implying effectively a full coverage at a 1000 GeV collider. In case of smuon pair production, as shown in the right plot of Fig. 3, energies up to  $\sim 1800$  GeV would be needed to fully cover the allowed parameter space.

All obtained cross-section predictions for the kinematically accessible parameter points are above  $10^{-2}$  pb for chargino production and above  $10^{-3}$  pb for smuon pair production. For each  $\text{ab}^{-1}$  of integrated luminosity this corresponds to 10000 (1000) events for chargino (smuon) pair production, which should make these particles easily accessible, see Tab. 1, if they are in the kinematic reach of the collider.

The above shown example cross-sections clearly show that at least some particles are guaranteed to be discovered at the higher-energy stages of the ILC and/or CLIC. If the



upcoming runs from the MUON G-2 experiment further confirm the deviation of  $a_\mu^{\text{exp}}$  from the SM prediction, the case for future  $e^+e^-$  colliders is clearly strengthened.

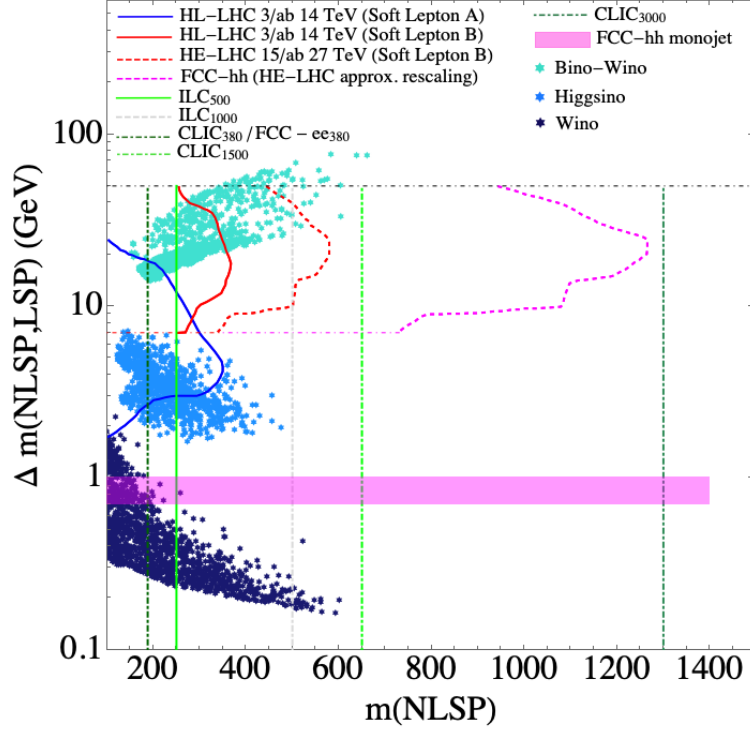


**Figure 4:**  $m_{\tilde{\chi}_1^\pm} - \Delta m$  plane with anticipated limits from compressed spectra searches at various future colliders, taken from Ref. [61]. Disappearing track searches are not included. Shown in blue, dark blue, turquoise are the points surviving all current constraints in the case of higgsino DM, wino DM and bino/wino DM with  $\tilde{\chi}_1^\pm$ -coannihilation, respectively, with relic density taken only as an upper limit.

In Fig. 4 we review the prospects at various high energy colliders for the compressed spectra searches, relevant for higgsino DM, wino DM and bino/wino DM with  $\tilde{\chi}_1^\pm$ -coannihilation [13]. We show our results in the  $m_{\tilde{\chi}_1^\pm} - \Delta m$  plane (with  $\Delta m := m_{\tilde{\chi}_1^\pm} - m_{\tilde{\chi}_1^0}$ ), which was presented (upto  $\Delta m = 0.7$  GeV) in Ref. [61] for the higgsino DM case, but also directly applicable for the wino DM case [55]. In addition to the anticipated limits from HL-LHC, HE-LHC and FCC-hh, we show the following projected limits from various high energy linear colliders sensitive up to the kinematic limit [61], looking at  $\tilde{\chi}_1^\pm \tilde{\chi}_1^\mp$  or  $\tilde{\chi}_2^0 \tilde{\chi}_1^0$  production (see also Ref. [55] and references therein)

- ILC with  $0.5 \text{ ab}^{-1}$  at  $\sqrt{s} = 500$  GeV (ILC500): solid light green.
- ILC with  $1 \text{ ab}^{-1}$  at  $\sqrt{s} = 1000$  GeV (ILC1000): gray dashed.
- CLIC with  $1 \text{ ab}^{-1}$  at  $\sqrt{s} = 380$  GeV (CLIC380): very dark green dot-dashed.
- CLIC with  $2.5 \text{ ab}^{-1}$  at  $\sqrt{s} = 1500$  GeV (CLIC1500): green dot-dashed.
- CLIC with  $5 \text{ ab}^{-1}$  at  $\sqrt{s} = 3000$  GeV (CLIC3000): dark green dot-dashed.

It can be observed that for the higgsino case, the HL-LHC can cover a part of the allowed parameter space, but an exhaustive coverage of the allowed parameter space can be reached only at a high-energy  $e^+e^-$  collider with  $\sqrt{s} \lesssim 1000$  GeV (i.e. ILC1000 or CLIC1500). For the wino DM, the  $\Delta m$  is so small that it largely escapes the HL-LHC searches (but may partially be detectable at the FCC-hh with monojet searches). As in the higgsino DM case, also here a high-energy  $e^+e^-$  collider will be necessary to cover the full allowed parameter space. While the currently allowed points would be covered by CLIC1500, a parameter space reduced further by e.g. the improved HL-LHC disappearing track searches, could be covered by the ILC1000. The bino/wino parameter points (turquoise) represent a more complicated case for the future collider analysis, since the limits assume a small mass difference between  $\tilde{\chi}_1^0$  and  $\tilde{\chi}_1^\pm$  as well as  $pp$  production cross sections for the higgsino case. For bino/wino DM case, these typically have larger production cross sections (so is the pure wino), i.e. application of these limits to the wino/bino points in Fig. 4 serves as conservative estimate for  $pp$  based limits. Consequently, it is expected that the HE-LHC or the FCC-hh would cover this scenario entirely. On the other hand, the  $e^+e^-$  limits should be directly applicable, and large parts of the parameter space will be effectively covered by the ILC1000, and the entire parameter space by CLIC1500.

Although we do not consider possibility of  $Z$  or  $h$  pole annihilation, it should be noted that in this context an LSP with  $M \sim m_{\tilde{\chi}_1^0} \sim M_Z/2$  or  $\sim M_h/2$  (with  $M = M_1$  or  $M_2$  or  $\mu$ ) would yield a detectable cross-section  $e^+e^- \rightarrow \tilde{\chi}_1^0 \tilde{\chi}_1^0 \gamma$  in any future high-energy  $e^+e^-$  collider. Furthermore, in the case of higgsino or wino DM, this scenario automatically yields other clearly detectable EW-SUSY signals at future  $e^+e^-$  colliders. For bino/wino DM this would depend on the values of  $M_2$  and/or  $\mu$ .

## Acknowledgments

I.S. thanks S. Matsumoto for the cluster facility. The work of I.S. is supported by World Premier International Research Center Initiative (WPI), MEXT, Japan. The work of S.H. is supported in part by the MEINCOP Spain under contract PID2019-110058GB-C21 and in part by the AEI through the grant IFT Centro de Excelencia Severo Ochoa SEV-2016-0597. The work of M.C. is supported by the project AstroCeNT: Particle Astrophysics Science and Technology Centre, carried out within the International Research Agendas programme of the Foundation for Polish Science financed by the European Union under the European Regional Development Fund.

## References

- [1] T. Aoyama *et al.*, [[arXiv:2006.04822](#) [hep-ph]].
- [2] M. Chakraborti, S. Heinemeyer and I. Saha, [[arXiv:2104.03287](#) [hep-ph]].
- [3] G. W. Bennett *et al.* [Muon g-2 Collaboration], *Phys. Rev. D* **73** (2006) 072003 [[hep-ex/0602035](#)].
- [4] J. Grange *et al.* [Muon g-2 Collaboration], [arXiv:1501.06858](#) [physics.ins-det].

- [5] B. Abi *et al.* [Muon  $g-2$ ], *Phys. Rev. Lett.* **126** (2021) no.14, 141801 doi:10.1103/PhysRevLett.126.141801 [[arXiv:2104.03281](#)] [hep-ex].
- [6] H. Nilles, *Phys. Rept.* **110** (1984) 1.
- [7] R. Barbieri, *Riv. Nuovo Cim.* **11** (1988) 1.
- [8] H. Haber, G. Kane, *Phys. Rept.* **117** (1985) 75.
- [9] J. Gunion, H. Haber, *Nucl. Phys. B* **272** (1986) 1.
- [10] H. Goldberg, *Phys. Rev. Lett.* **50** (1983) 1419.
- [11] J. Ellis, J. Hagelin, D. Nanopoulos, K. Olive, M. Srednicki, *Nucl. Phys. B* **238** (1984) 453.
- [12] M. Chakraborti, S. Heinemeyer and I. Saha, *Eur. Phys. J. C* **80** (2020) 10, 984 [[arXiv:2006.15157](#)] [hep-ph].
- [13] M. Chakraborti, S. Heinemeyer and I. Saha, [arXiv:2103.13403](#) [hep-ph].
- [14] M. Drees, H. Dreiner, D. Schmeier, J. Tattersall and J. S. Kim, *Comput. Phys. Commun.* **187** (2015), 227-265 [[arXiv:1312.2591](#)] [hep-ph].
- [15] J. S. Kim, D. Schmeier, J. Tattersall and K. Rolbiecki, *Comput. Phys. Commun.* **196** (2015), 535-562 [[arXiv:1503.01123](#)] [hep-ph].
- [16] D. Dercks, N. Desai, J. S. Kim, K. Rolbiecki, J. Tattersall and T. Weber, *Comput. Phys. Commun.* **221** (2017), 383-418 [[arXiv:1611.09856](#)] [hep-ph].
- [17] H. Baer *et al.*, *The International Linear Collider Technical Design Report - Volume 2: Physics*, [arXiv:1306.6352](#) [hep-ph].
- [18] G. Moortgat-Pick *et al.*, *Eur. Phys. J. C* **75** (2015) 8, 371 [[arXiv:1504.01726](#)] [hep-ph].
- [19] L. Linssen, A. Miyamoto, M. Stanitzki and H. Weerts, [arXiv:1202.5940](#) [physics.ins-det];  
H. Abramowicz *et al.* [CLIC Detector and Physics Study Collaboration], [arXiv:1307.5288](#) [hep-ex];  
P. Burrows *et al.* [CLICdp and CLIC Collaborations], *CERN Yellow Rep. Monogr.* **1802** (2018) 1 [[arXiv:1812.06018](#)] [physics.acc-ph].
- [20] See: <https://twiki.cern.ch/twiki/bin/view/AtlasPublic/SupersymmetryPublicResults> .
- [21] See: <https://twiki.cern.ch/twiki/bin/view/CMSPublic/PhysicsResultsSUS> .
- [22] E. Bagnaschi *et al.*, *Eur. Phys. J. C* **78** (2018) no.3, 256 [[arXiv:1710.11091](#)] [hep-ph].
- [23] P. Slavich, S. Heinemeyer (eds.), E. Bagnaschi *et al.*, [arXiv:2012.15629](#) [hep-ph].

- [24] M. Carena, J. Osborne, N. R. Shah and C. E. M. Wagner, *Phys. Rev. D* **98** (2018) no.11, 115010 doi:10.1103/PhysRevD.98.115010 [[arXiv:1809.11082](#) [hep-ph]].
- [25] S. Borsanyi *et al.*, [arXiv:2002.12347](#) [hep-lat].
- [26] C. Lehner and A. S. Meyer, *Phys. Rev. D* **101** (2020), 074515 [[arXiv:2003.04177](#) [hep-lat]].
- [27] A. Crivellin, M. Hoferichter, C. A. Manzari and M. Montull, *Phys. Rev. Lett.* **125** (2020) no.9, 091801 [[arXiv:2003.04886](#) [hep-ph]].
- [28] A. Keshavarzi, W. J. Marciano, M. Passera and A. Sirlin, *Phys. Rev. D* **102** (2020) no.3, 033002 [[arXiv:2006.12666](#) [hep-ph]].
- [29] P. Athron *et al.*, *Eur. Phys. J. C* **76** (2016) no.2, 62 [[arXiv:1510.08071](#) [hep-ph]].
- [30] P. von Weitershausen, M. Schafer, H. Stockinger-Kim and D. Stockinger, *Phys. Rev. D* **81** (2010), 093004 [[arXiv:1003.5820](#) [hep-ph]].
- [31] H. Fargnoli, C. Gnendiger, S. Paßehr, D. Stöckinger and H. Stöckinger-Kim, *JHEP* **1402** (2014), 070 [[arXiv:1311.1775](#) [hep-ph]].
- [32] M. Bach, J. h. Park, D. Stöckinger and H. Stöckinger-Kim, *JHEP* **1510** (2015), 026 [[arXiv:1504.05500](#) [hep-ph]].
- [33] S. Heinemeyer, D. Stockinger and G. Weiglein, *Nucl. Phys. B* **690** (2004), 62-80 [[arXiv:hep-ph/0312264](#) [hep-ph]].
- [34] S. Heinemeyer, D. Stockinger and G. Weiglein, *Nucl. Phys. B* **699** (2004), 103-123 [[arXiv:hep-ph/0405255](#) [hep-ph]].
- [35] W. G. Hollik, G. Weiglein and J. Wittbrodt, *JHEP* **03** (2019), 109 [[arXiv:1812.04644](#) [hep-ph]].
- [36] T. Robens, T. Stefaniak and J. Wittbrodt, *Eur. Phys. J. C* **80** (2020) no.2, 151 [[arXiv:1908.08554](#) [hep-ph]].
- [37] M. Aaboud *et al.* [ATLAS Collaboration], *JHEP* **06** (2018), 022 [[arXiv:1712.02118](#) [hep-ex]].
- [38] A. M. Sirunyan *et al.* [CMS Collaboration], *Phys. Lett. B* **806** (2020), 135502 [[arXiv:2004.05153](#) [hep-ex]].
- [39] N. Aghanim *et al.* [Planck Collaboration], [arXiv:1807.06209](#) [astro-ph.CO].
- [40] G. Belanger, F. Boudjema, A. Pukhov and A. Semenov, *Comput. Phys. Commun.* **149** (2002), 103-120 [[arXiv:hep-ph/0112278](#) [hep-ph]].
- [41] G. Belanger, F. Boudjema, A. Pukhov and A. Semenov, *Comput. Phys. Commun.* **176** (2007), 367-382 [[arXiv:hep-ph/0607059](#) [hep-ph]].

- [42] G. Belanger, F. Boudjema, A. Pukhov and A. Semenov, *Comput. Phys. Commun.* **177** (2007), 894-895.
- [43] G. Belanger, F. Boudjema, A. Pukhov and A. Semenov, [arXiv:1305.0237](#) [hep-ph].
- [44] E. Aprile *et al.* [XENON Collaboration], *Phys. Rev. Lett.* **121** (2018) no.11, 111302 [[arXiv:1805.12562](#) [astro-ph.CO]].
- [45] A. Djouadi, J. L. Kneur and G. Moultaka, *Comput. Phys. Commun.* **176** (2007) 426 [[hep-ph/0211331](#)].
- [46] Joint LEP2 SUSY Working Group, the ALEPH, DELPHI, L3 and OPAL Collaborations, see: <http://lepsusy.web.cern.ch/lepsusy/>.
- [47] M. Muhlleitner, A. Djouadi and Y. Mambrini, *Comput. Phys. Commun.* **168** (2005) 46 [[hep-ph/0311167](#)].
- [48] G. Aad *et al.* [ATLAS Collaboration], *Phys. Rev. D* **101** (2020) no.5, 052005 [[arXiv:1911.12606](#) [hep-ex]].
- [49] G. Aad *et al.* [ATLAS Collaboration], *Eur. Phys. J. C* **80** (2020) no.2, 123 [[arXiv:1908.08215](#) [hep-ex]].
- [50] S. Heinemeyer and C. Schappacher, *Eur. Phys. J. C* **77** (2017) no.9, 649 [[arXiv:1704.07627](#) [hep-ph]].
- [51] S. Heinemeyer and C. Schappacher, *Eur. Phys. J. C* **78** (2018) no.7, 536
- [52] T. Fritzsche, T. Hahn, S. Heinemeyer, F. von der Pahlen, H. Rzehak and C. Schappacher, *Comput. Phys. Commun.* **185** (2014), 1529-1545 [[arXiv:1309.1692](#) [hep-ph]].
- [53] M. Berggren, [[arXiv:1308.1461](#) [hep-ph]].
- [54] M. T. N. Pardo de Vera, M. Berggren and J. List, [[arXiv:2002.01239](#) [hep-ph]].
- [55] M. Berggren, [[arXiv:2003.12391](#) [hep-ph]].
- [56] H. Baer, M. Berggren, K. Fujii, J. List, S. L. Lehtinen, T. Tanabe and J. Yan, *Phys. Rev. D* **101** (2020) no.9, 095026 [[arXiv:1912.06643](#) [hep-ex]].
- [57] T. Barklow, J. Brau, K. Fujii, J. Gao, J. List, N. Walker and K. Yokoya, [[arXiv:1506.07830](#) [hep-ex]].
- [58] K. Fujii *et al.*, [[arXiv:1710.07621](#) [hep-ex]].
- [59] A. Robson and P. Roloff, [[arXiv:1812.01644](#) [hep-ex]].
- [60] J. de Blas *et al.*, *JHEP* **01** (2020), 139 [[arXiv:1905.03764](#) [hep-ph]].
- [61] R. K. Ellis *et al.* [[arXiv:1910.11775](#) [hep-ex]].